# The influence of excess $K_2O$ on the electrical properties of $(K,Na)_{1/2}Bi_{1/2}TiO_3$ ceramics

Linhao Li[1], Ming Li[2] and Derek C Sinclair[1,a)]

[1]1. Department of Materials Science and Engineering, University of Sheffield, Mappin Street, Sheffield, S1 3JD, UK

2. Department of Mechanical, Materials and Manufacturing Engineering, University of Nottingham, University Park, Nottingham, NG7 2RD, UK

**Abstract**

The solid solution $(K_xNa_{0.50-x})Bi_{0.50}TiO_3$ (KNBT) between $Na_{1/2}Bi_{1/2}TiO_3$ (NBT) and $K_{1/2}Bi_{1/2}TiO_3$ (KBT) has been extensively researched as a candidate lead-free piezoelectric material because of its relatively high Curie temperature and good piezoelectric properties, especially near the morphotropic phase boundary (MPB) at x ~ 0.10 (20 mol% KBT). Here we show low levels of excess $K_2O$ in the starting compositions, i.e. $(K_{y+0.03}Na_{0.50-y})Bi_{0.50}TiO_{3.015}$ (y-series), can significantly change the conduction mechanism and electrical properties compared to a nominally stoichiometric KNBT series $(K_xNa_{0.50-x})Bi_{0.50}TiO_3$ (x-series). Impedance Spectroscopy measurements reveal significantly higher bulk conductivity ($\sigma_b$) values for y ≥ 0.10 samples (activation energy, $E_a$, ≤ 0.95 eV) compared to the corresponding x-series samples which possess band-gap type electronic conduction ($E_a$ ~ 1.26 to 1.85 eV). The largest difference in electrical properties occurs close to the MPB composition (20 mol% KBT) where y = 0.10 ceramics possess $\sigma_b$ (at 300 °C) that is 4 orders of magnitude higher than x = 0.10 and the oxide-ion transport number in the former is ~ 0.70 – 0.75 compared to < 0.05 in the latter (between 600 and 800 °C). The effect of excess $K_2O$ can be rationalised on the basis of the (K + Na):Bi ratio in the starting composition prior to ceramic processing. This demonstrates the electrical properties of KNBT to be sensitive to low levels of A-site nonstoichiometry and indicates excess $K_2O$ in KNBT starting compositions to compensate for volatilisation can lead to undesirable high dielectric loss and leakage currents at elevated temperatures.

[a)]Electronic mail: d.c.sinclair@sheffield.ac.uk.

Piezoelectric ceramics have been extensively used in applications such as actuators, sensors, and transducers since the 1950's due to their excellent electro-mechanical properties. Among all oxides, lead zirconate titanate ($Pb(Zr_{1-x}Ti_x)O_3$, PZT) has been the most widely investigated and used piezoelectric material; however, with growing concerns about the toxicity of lead, research on more environment-friendly, lead-free replacements for PZT has become imperative. Sodium bismuth titanate ($Na_{1/2}Bi_{1/2}TiO_3$, NBT), potassium bismuth titanate ($K_{1/2}Bi_{1/2}TiO_3$, KBT) and their solid solutions with each other and with other Pb-free ferroelectric perovskites such as $BaTiO_3$ are considered as promising candidates due to their relatively high Curie temperatures and competitive piezoelectric properties. [1–8] A common feature of PZT, KBT and NBT is the volatility of the A-site cations during high temperature processing. In order to maintain charge balance, in some cases such volatility (e.g. Pb in PZT and Bi in NBT) can introduce oxygen vacancies which can lead to high levels of dielectric loss via oxide-ion or electronic conduction. Therefore it is common practice to add excess levels of A-site cation reagents in starting compositions in attempts to compensate for their volatility.

In recent years we have demonstrated the electrical behaviour of NBT to be highly sensitive to low levels of A-site non-stoichiometry[9–12] with three different types of conduction being identified depending on the A-site starting composition. Type I NBT with a starting Na:Bi ratio ≥1 possess high oxide-ion conduction (oxide-ion transport number, $t_{ion} > 0.85$) which is comparable to/slightly lower than the best known oxide-ion conductors such as gadolinia-doped ceria (GDC) and yttria-stabilised zirconia (YSZ); type II with Na:Bi << 1 are mixed oxide-ion and n-type electronic conductors ($0.2 < t_{ion} < 0.6$); type III with Na:Bi < 1 are excellent dielectric materials that exhibit near intrinsic electronic conduction ($t_{ion} < 0.1$) and low dielectric loss.[11] The difference in bulk conductivity between type I and III NBTs can be more than three orders of magnitude. In addition to A-site non-stoichiometry, the level of oxygen vacancies can also be suppressed by donor (e.g. $Nb^{5+}$ for $Ti^{4+}$) dopants or further enhanced by acceptor (e.g. $Mg^{2+}$ for $Ti^{4+}$ or $Sr^{2+}$ for $Bi^{3+}$) dopants, which can be employed to manipulate the level of oxide-ion conduction in NBT.[13–16]

In contrast to NBT, the electrical properties of KBT do not exhibit such a strong dependence on the starting A-site non-stoichiometry. Although KBT can exhibit mixed oxide-ion/electronic conduction

at high temperatures (> 600 °C)[17], the level of oxide-ion conduction in KBT is rather low compared to NBT (~ 3 orders of magnitude lower). Although not fully understood, this has been attributed to the difference in polymorphism exhibited by these perovskites. Compared to NBT, KBT has the Na ion replaced by the larger K ion, which increases the tolerance factor and leads to a non-tilted perovskite-type structure. It is also noteworthy that below ~ 300 °C, KBT exhibits a significant level of volumetric proton conduction which is sensitive to the K content in the starting composition with higher K contents leading to higher levels of proton conduction[17]. Considering these differences, it is interesting to examine the binary solid solution between these two compounds.

The KBT-NBT solid solution (KNBT) is one of the candidates for lead-free piezoelectric ceramics. It has attracted interest because of its high permittivity and good electromechanical properties, especially at 16 ~ 20mol% KBT where there is a reported morphotropic phase boundary (MPB) between the room temperature rhombohedral (NBT) and tetragonal (KBT) structured end members.[8,18–21] However, unlike NBT, most dielectric studies performed on KNBT show good dielectric properties with low dielectric loss (tan δ), despite the high oxide-ion conduction that can occur in NBT.[18,22,23] Here we investigate the electrical conduction mechanism(s) within the KNBT solid solution to improve our understanding of the structure–composition–property relationships not only for this solid solution but also for the two end members. In particular, we report on the influence of the K-content in the starting composition on the electrical properties of KNBT via two series of ceramics: nominally stoichiometric $(K_xNa_{0.50-x})Bi_{0.50}TiO_3$ ($0.00 \le x \le 0.50$, x-series) and K-excess $(K_{y+0.03}Na_{0.50-y})Bi_{0.50}TiO_{3.015}$ ($0.10 \le y \le 0.50$, y-series).

$(K_xNa_{0.50-x})Bi_{0.50}TiO_3$ ($0.00 \le x \le 0.50$, x-series) and $(K_{y+0.03}Na_{0.50-y})Bi_{0.50}TiO_{3.015}$ ($0.10 \le y \le 0.50$, y-series) ceramics were prepared by the conventional solid-state method. The mixtures of raw materials $Na_2CO_3$ (99.5%), $K_2CO_3$ (99.5%), $Bi_2O_3$ (99.9%) and $TiO_2$ (99.9%) were ball milled for 6 h, dried, sieved, and calcined at 800 °C for 2 h. The resultant powders were ball milled for 4 h followed by another 2 h calcination at 850 ~ 900 °C and another 6 h ball milling. Pellets were sintered at 1050-1150 °C for 2 h. The phase purity, polymorphism, microstructure and chemical composition of the sintered ceramics were determined by a combination of X-ray powder diffraction (XRD), scanning electron microscopy (SEM) and energy dispersive X-ray spectroscopy (EDX). The electrical

properties were determined by Impedance Spectroscopy (IS). Oxide-ion transport number measurements (EMF) were performed on a ProboStat system. More details can be found in Supplementary Material.

XRD data (Fig S1, Supplementary Material) showed a complete solid solution between NBT and KBT with no extra peaks observed from any secondary phase for both KNBT x and y series; however, SEM/EDX data (Fig S2, Supplementary Material) revealed small amounts of $K_2Ti_6O_{13}$ (identification based on EDX data) as a secondary phase in x and y = 0.50. The calculated lattice parameters (Fig S1, Supplementary Material) for the KNBT ceramics from XRD data showed a continuous increase with increasing KBT content therefore confirming the existence of a near complete solid solution between the end member phases. The grain size of the KNBT ceramics decreased significantly with the KBT content from about 5 ~ 10 μm for x = 0.00 to 0.5 ~ 1 μm for x and y = 0.10, (Fig S3, Supplementary Material). The density of sintered ceramics (Fig S4, Supplementary Material) decreased with increasing KBT content and most notably from > 90 % for x or y ≤ 0.20 to ~ 70 – 85 % for x or y ≥ 0.30. Low ceramic density does not significantly influence the magnitude of the bulk conductivity extracted from IS data and therefore allows comparison of conductivity trends across both series. In contrast, the dielectric properties are strongly influenced by porosity and therefore dielectric data are only shown for x and y = 0.10 where ceramic density was> 95% of the theoretical X-ray density.

Impedance complex plane (Z*) plots for the x- and y-series ceramics at 600 $^oC$ are shown in Figure 1. A single arc was observed in the measured frequency range for all samples except x = 0.00, 0.02 and y = 0.10. On the other hand, the x = 0.00 and 0.02 data consist of an incomplete higher frequency arc, a distorted lower frequency arc and a low frequency (< 1 Hz) electrode-type response, Fig 1(b), whereas data for y = 0.10 consisted of a single incomplete arc with a low frequency electrode-type response, Fig 1(d). The associated capacitance for the high frequency arc (single arc in most cases) for all ceramics in both series was in the range of 52 ~ 147 pF/cm at 600 $^oC$ which is consistent with the grain (bulk) response. In general, the bulk resistivity ($R_b$) increased with x and y for all KNBTs; however, the trend is clearly different between the two series. In the x-series, $R_b$ can be separated into two different groups, i.e., x = 0.00, 0.02 and the rest of the series.

At 600 °C, it increases initially from ~ 600 Ω•cm for x = 0.00 to ~ 2.5 kΩ•cm for x = 0.02, Fig 1(b). When the KBT content is increased to 20mol% (x = 0.10), $R_b$ dramatically increases to ~ 150 kΩ•cm and remains in the range of ~ 150 – 620 kΩ•cm with no clear trend for x ≥ 0.10, Figure 1 (a). In contrast, there is a less dramatic increase in $R_b$ for the y-series, Fig 1 (c) and (d). $R_b$ for y = 0.10 was only ~4.8 kΩ•cm which further increased with KBT content with a maximum value of ~420 kΩ•cm obtained for y = 0.40, Fig 1(c).

Comparing the x and y KNBT series, samples with 20 mol% KBT (i.e. x and y = 0.10) display the largest difference in electrical properties. $R_b$ of x = 0.10 is about 2 orders of magnitude higher than y = 0.10 (e.g. $R_b$ ~ 150 kΩ•cm for x = 0.10 and ~ 4.8 kΩ•cm for y = 0.10 at 600 °C, Figs 1 (a) and 1(d), respectively). In addition, a low frequency spike in the Z* plot for y = 0.10 is consistent with Warburg diffusion and indicates a significant level of oxide-ion conduction in this sample, Fig 1(d) inset which is not present in x = 0.10, Fig 1(a).

The temperature dependence of the bulk conductivity, $\sigma_b$ (where $\sigma_b = 1/R_b$) for all samples is summarised in an Arrhenius plot in Figure 2. For the x-series, $\sigma_b$ is sensitive to relatively low levels of KBT and decreases by more than three orders of magnitude for x ≥ 0.10, Fig 2 (a); whereas for the y-series $\sigma_b$ decreased gradually with increasing KBT content, Fig 2 (b). It is noteworthy that the activation energy ($E_a$) for $\sigma_b$ for these two series of samples are also significantly different. For the x-series, $E_a$ changes from ≤ 0.85 eV for x ≤ 0.02 to ~ 1.26 to 1.85 eV for x ≥ 0.10 indicating a change in conduction mechanism. In contrast, $E_a$ remains relatively low and similar for all samples in the y-series (< 0.95 eV).

The 1.5 mol% extra $K_2O$ in the starting composition of y = 0.10 had a modest influence on the magnitude and temperature of the relative permittivity maximum ($\varepsilon_{r,max}$) which was ~ 5820 at ~ 300 °C for x = 0.10 and ~ 5480 at 290 °C for y = 0.10. In contrast, it had a dramatic effect on tan δ: y = 0.10 exhibited high levels of dielectric loss (> 0.15) above ~ 400 °C whereas x = 0.10 displayed low loss (< 0.01) in the temperature range 320 ~ 500 °C, Fig 3. The loss maximum observed at <300 °C shifts from ~ 108 °C for x = 0.10 to ~ 240 °C for y = 0.10.

The change in conduction mechanism of the x-series but not in the y-series of samples was confirmed by EMF measurements using air/nitrogen gas, Fig 4. A significant level of oxide-ion conduction was observed for y = 0.10 with an ionic transport number ($t_{ion}$) ~ 0.70 to 0.75 from 600

to 800 °C. In contrast, $t_{ion}$ for x = 0.10 was less than 0.05 indicating the predominant conduction mechanism had switched from oxide-ion to electronic conduction. This is in agreement with the change of $E_a$ in $\sigma_b$ for the x-series, Fig 2 (a).

The IS, LCR and EMF data reveal the electrical behaviour of the two series of KNBT samples in this study to be different, Figs 1 to 4. The x-series with x ≥ 0.10 exhibit excellent dielectric behaviour consistent with Type III NBT with low $\sigma_b$ and high associated $E_a$, low $t_{ion}$ and low dielectric loss above 300 °C. In contrast, the y–series (1.5 mol% excess $K_2O$ in the starting composition) possess mixed ionic-electronic Type II NBT behaviour with relatively high $\sigma_b$ with lower associated $E_a$, significant $t_{ion}$ and high dielectric loss above 300 °C which is consistent with significant levels of oxide-ion conduction. Clearly, the 1.5 mol% extra $K_2O$ in the starting compositions of the y-series leads to the difference in electrical behaviour.

The electrical properties of NBT are known to be highly sensitive to low level of A-site non-stoichiometry in the starting composition.[12] Nominally stoichiometric NBT, Bi-deficient or Na-excess starting compositions (under our processing conditions) all produce type I oxide-ion conduction behaviour whereas slightly Bi-excess (< 2 mol%) or Na-deficient starting compositions can supress the oxide-ion conduction and lead to type III insulating behaviour.[9,10] It is worthy to note that the defect mechanisms for Na and Bi non-stoichiometry in NBT are different and can lead to opposite effects in their electrical properties. The most important parameter in controlling which defect mechanism will be adopted is the A-site Na:Bi ratio in the nominal starting composition. Starting compositions with Na:Bi ≥ 1 lead to the formation of oxygen vacancies in NBT and secondary phase(s) whereas starting compositions with Na:Bi < 1 lead only to the formation of secondary phase(s) without formation of significant levels of oxygen vacancies in NBT. In addition, it is now well known that the electrical properties of nominally stoichiometric NBT are strongly dependent on processing procedures such as the drying of raw materials prior to batching the powders for calcination and for covering pellets with sacrificial powder during sintering. Thus, the ratio of $Na_2O$- to $Bi_2O_3$-loss during ceramic processing is critical to the electrical properties of nominally stoichiometric NBT as it can influence the Na:Bi ratio in sintered ceramics. Under our processing conditions, stoichiometric NBT is always a type I oxide ion conductor due to the loss of

more $Bi_2O_3$ than $Na_2O$ during processing. This results in an A-site Na:Bi > 1 and creates oxygen vacancies that produces the oxide-ion conduction in NBT.

In this study, the stoichiometric KNBTs (x-series samples) with x ≥ 0.10 behave like type III insulating NBTs, Fig 2 (a). We attribute this rapid change in behaviour to a difference in the volatility of $Na_2O$ and $K_2O$ with $K_2O$ being easier to volatilise during processing. If the loss of $Bi_2O_3$ in nominally stoichiometric NBT can be partially compensated by the loss of $K_2O$ such that (K + Na):Bi is closer to unity then $\sigma_b$ will be reduced due to a decrease in oxide vacancy concentration as in the case of x = 0.02, Fig 2 (a). With increasing K content in the starting compositions for both series, the loss of $K_2O$ will be similar or surpass the loss of $Bi_2O_3$ during processing such that the composition of the perovskite phase in the KNBT ceramics will essentially be (K + Na):Bi ≤ 1. Based on previous results for NBT, it is known that starting compositions with Na:Bi < 1 have a low level of oxygen vacancies and this leads to type III insulating behaviour as observed for x ≥ 0.10, Fig 2 (a). This suggestion is confirmed by the y-series results. In this case, the loss of $K_2O$ during processing is partially compensated by the 1.5 mol% excess $K_2O$ in the starting compositions. The y-series are effectively nominally Bi-deficient due to the adjustment of (K+Na):Bi > 1 and although loss of $K_2O$, $Na_2O$ and $Bi_2O_3$ occur during processing, this starting ratio is sufficient to ensure the formation of oxygen vacancies and therefore oxide-ion conductivity, especially for y = 0.10, Fig 2 (b) and 4.

Despite the excess $K_2O$ in the nominal starting composition of the y-series to compensate for K-loss during processing, $\sigma_b$ for the y-series still decreases with increasing K-content; however, $E_a$ remains unchanged. Combined with the modest decrease of $t_{ion}$ when compared to NBT, Fig 4, this suggests the decrease in $\sigma_b$ for the y-series is associated with a decrease in the charge carrier concentration rather than a change in conduction mechanism. This decreasing of charge carrier concentration is related either a small change in the (K + Na):Bi ratio across the y-series or possibly to subtle, local structural changes associated with K doping in NBT. NBT exhibits a complex in-phase and out-of-phase $TiO_6$ tilted structure with off-centred and underbonded Bi ions.[24–27] This leads to weak Bi–O bonding which plays a crucial role in the oxide-ion conduction in NBT. Such tilting of octahedra are reduced when the smaller Na ion is replaced by the larger K ion and result in a non-tilted system for KBT contents ≥ 50 mol%.[19] The reduction of tilting will homogenise the Bi–O bond

lengths which eventually strengthen the Bi–O bonding and reduce the concentration of mobile oxide ions (i.e. charge carrier concentration).

Unlike NBT, there are no reports of KNBT solid solutions being 'leaky' which means the insulating behaviour of the stoichiometric KNBTs (x-series) is reproducible and the loss of (K + Na) during processing is surpassing the loss of Bi under different experimental conditions to ensure (K + Na):Bi is < 1 in the perovskite lattice of sintered ceramics.[28-35] KNBTs therefore always possess insulating behaviour unless extra K is intentionally added into the starting composition to compensate for the loss such that (K+Na):Bi ≥ 1, as in the y-series. It is noteworthy that, as a candidate lead-free piezoelectric material, the best piezoelectric and dielectric properties in the NBT-KBT solid solution have been reported near the MPB which is located at 16 ~ 20 mol% KBT. In this study, the largest difference in bulk conductivity and dielectric loss between the two series of samples occurred at ~ 20 mol% KBT (i.e. x and y = 0.10). Diligence is therefore required when developing devices or conducting research based on the reported NBT-KBT MPB as small changes of the K content in the starting material may dramatically alter the dielectric loss properties of the final product, Fig 3. In the case of KNBT, adding an excess of $K_2CO_3$ to compensate for volatilisation is not recommended for high temperature dielectric/piezoelectric applications as this can adjust the (K + Na):Bi ratio to exceed unity and result in high levels of tan $\delta$ above 300 $^{o}$C due to significant levels of oxide-ion conductivity.

See supplementary material for detailed experimental procedure, XRD, SEM, lattice parameter and ceramic density results.

We thank the EPSRC for funding (EP/L027348/1).

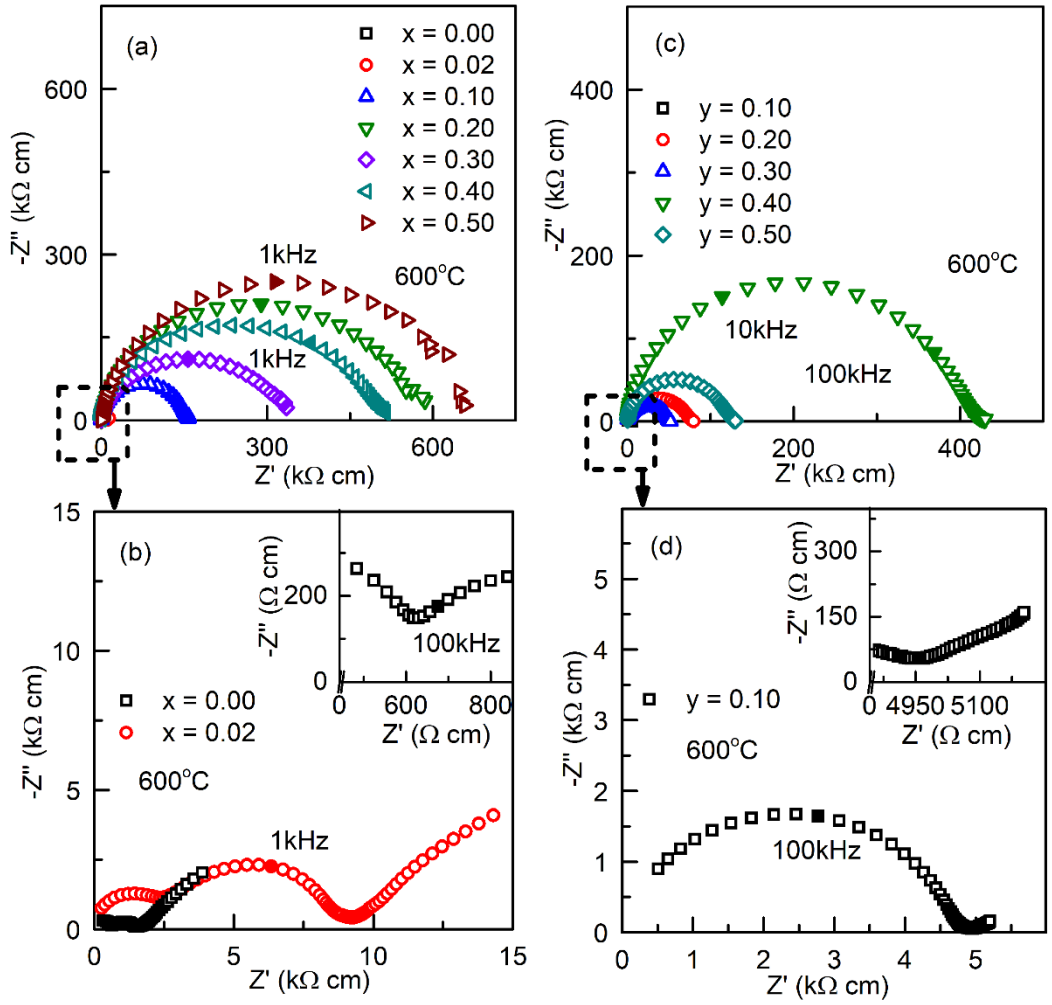


Figure 1. Z* plots of (a) $(K_xNa_{0.50-x})Bi_{0.50}TiO_3$ and (c) $(K_{y+0.03}Na_{0.50-y})Bi_{0.50}TiO_{3.015}$ series samples at 600 °C. (b), (d) High-frequency data of (a) and (c) on an expanded scale, respectively; Inset in (b) shows the bulk response for x = 0.00; inset in (d) shows the low-frequency data for y = 0.10.

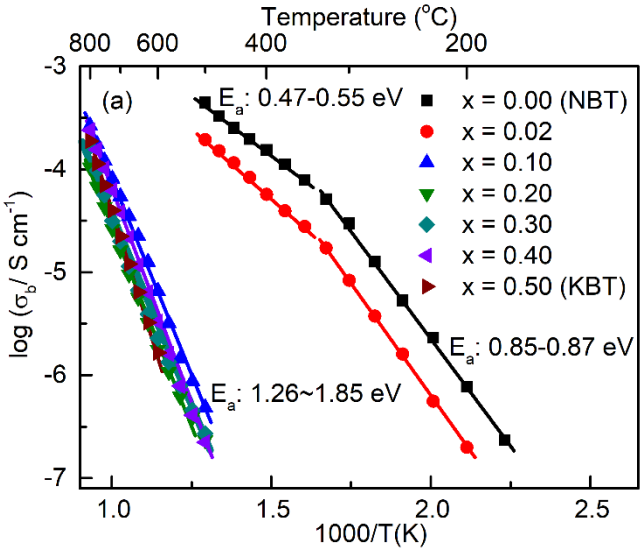

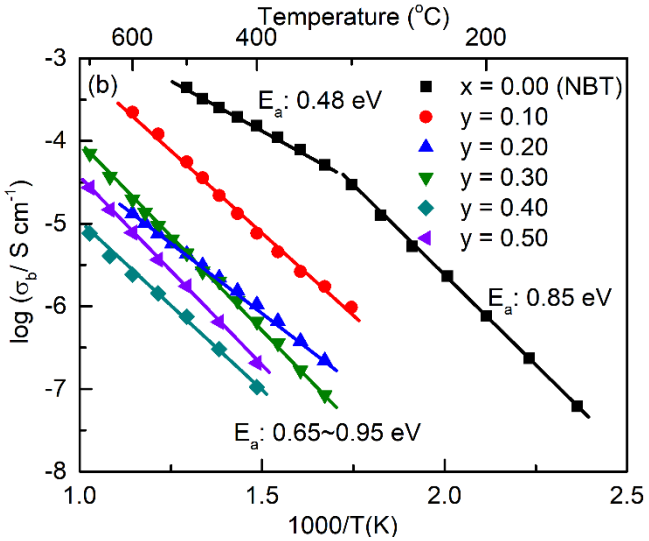


Figure 2. Arrhenius-type plots of bulk conductivity for (a) $(K_xNa_{0.50-x})Bi_{0.50}TiO_3$ and (b) $(K_{y+0.03}Na_{0.50-y})Bi_{0.50}TiO_{3..015}$ series.

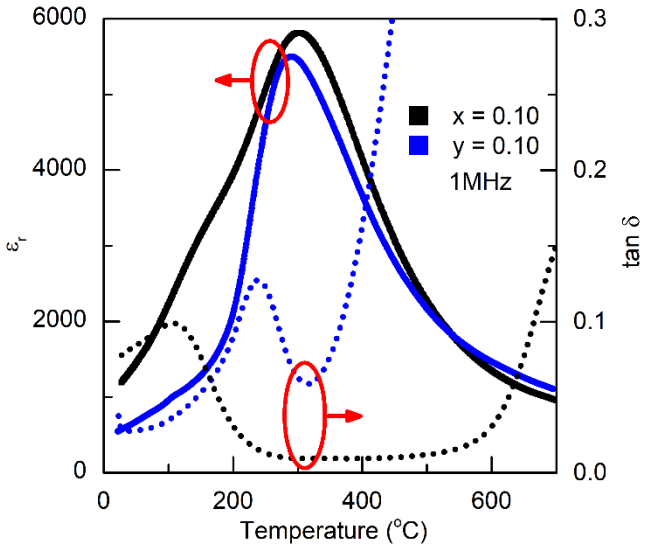


Figure 3. Temperature dependence of $\varepsilon_r$ (solid lines) and tan δ (dashed lines) at 1 MHz for $(K_{0.10}Na_{0.40})Bi_{0.50}TiO_3$ (x = 0.10) and $(K_{0.13}Na_{0.40})Bi_{0.50}TiO_{3.015}$ (y = 0.10).

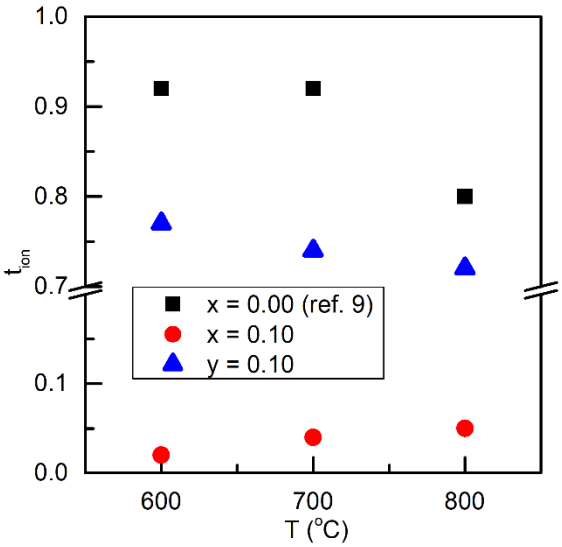


Figure 4. Oxygen ionic transport number, $t_{ion}$, for $(K_{0.10}Na_{0.40})Bi_{0.50}TiO_3$ (x = 0.10) and $(K_{0.13}Na_{0.40})Bi_{0.50}TiO_{3.015}$ (y = 0.10) from EMF measurements using air/nitrogen gas.

**References**

[1] Y. Saito, H. Takao, T. Tani, T. Nonoyama, K. Takatori, T. Homma, T. Nagaya, and M. Nakamura, Nature **432**, 84 (2004).

[2] J. Rödel, K.G. Webber, R. Dittmer, W. Jo, M. Kimura, and D. Damjanovic, J. Eur. Ceram. Soc. **35**, 1659 (2015).

[3] J. Rödel, W. Jo, K.T.P. Seifert, E.M. Anton, T. Granzow, and D. Damjanovic, J. Am. Ceram. Soc. **92**, 1153 (2009).

[4] Y. Hiruma, R. Aoyagi, H. Nagata, and T. Takenaka, Jpn. J. Appl. Phys. **44**, 5040 (2005).

[5] S.M. Emel'yanov, I.P. Raevskii, F.I. Savenko, Y.M. Popov, S.M. Zaitsev, and N.S. Mazankina, Sov. Phys. Solid State **29**, 1446 (1987).

[6] S.M. Emel'yanov, I.P. Raevskii, and O.I. Prokopalo, Sov. Phys. Solid State **25**, 889 (1983).

[7] H. Nagata, M. Yoshida, Y. Makiuchi, and T. Takenaka, Japanese J. Appl. Physics, Part 1 Regul. Pap. Short Notes Rev. Pap. **42**, 7401 (2003).

[8] A. Sasaki, T. Chiba, Y. Mamiya, and E. Otsuki, Jpn. J. Appl. Phys. **38**, 5564 (1999).

[9] M. Li, M.J. Pietrowski, R. a De Souza, H. Zhang, I.M. Reaney, S.N. Cook, J.A. Kilner, and D.C. Sinclair, Nat. Mater. **13**, 31 (2014).

[10] M. Li, H. Zhang, S.N. Cook, L. Li, J.A. Kilner, I.M. Reaney, and D.C. Sinclair, Chem. Mater. **27**, 629

(2015).

[11] L. Li, M. Li, H. Zhang, I.M. Reaney, and D.C. Sinclair, J. Mater. Chem. C **4**, 5779 (2016).

[12] F. Yang, M. Li, L. Li, P. Wu, E. Pradal-Velázquez, and D.C. Sinclair, J. Mater. Chem. A (2018). DOI: 10.1039/C7TA09245H

[13] M. Li, L. Li, J. Zang, and D.C. Sinclair, Appl. Phys. Lett. **106**, 102904 (2015).

[14] F. Yang, P. Wu, and D.C. Sinclair, Solid State Ionics **299**, 38 (2017).

[15] F. Yang, H. Zhang, L. Li, I.M. Reaney, and D.C. Sinclair, Chem. Mater. **28**, 5269 (2016).

[16] F. Yang, M. Li, L. Li, P. Wu, E. Pradal-Velázque, and D.C. Sinclair, J. Mater. Chem. A **5**, 21658 (2017).

[17] L. Li, M. Li, I.M. Reaney, and D.C. Sinclair, J. Mater. Chem. C **5**, 6300 (2017).

[18] O. Elkechai, M. Manier, and J.P. Mercurio, Phys. Status Solidi **157**, 499 (1996).

[19] G.O. Jones, J. Kreisel, and P.A. Thomas, Powder Diffr. **17**, 301 (2002).

[20] V.A. Shuvaeva, D. Zekria, A.M. Glazer, Q. Jiang, S.M. Weber, P. Bhattacharya, and P.A. Thomas, Phys. Rev. B **71**, 174114 (2005).

[21] J. Kreisel, A.M. Glazer, G. Jones, P.A. Thomas, L. Abello, and G. Lucazeau, J. Phys. Condens. Matter **12**, 3267 (2000).

[22] M. Otoničar, S.D. Škapin, M. Spreitzer, and D. Suvorov, J. Eur. Ceram. Soc. **30**, 971 (2010).

[23] T. Kainz, M. Naderer, D. Schütz, O. Fruhwirth, F. a. Mautner, and K. Reichmann, J. Eur. Ceram. Soc. **34**, 3685 (2014).

[24] G.O. Jones and P.A. Thomas, Acta Crystallogr. Sect. B Struct. Sci. **58**, 168 (2002).

[25] E. Aksel, J.S. Forrester, J.L. Jones, P.A. Thomas, K. Page, and M.R. Suchomel, Appl. Phys. Lett. **98**, 152901 (2011).

[26] V. Dorcet, G. Trolliard, and P. Boullay, Chem. Mater. **77**, 5061 (2008).

[27] I. Levin and I.M. Reaney, Adv. Funct. Mater. **22**, 3445 (2012).

[28] W. Chen, Y. Li, Q. Xu, and J. Zhou, J. Electroceramics **15**, 229 (2005).

[29] Y. Li, W. Chen, Q. Xu, J. Zhou, X. Gu, and S. Fang, Mater. Chem. Phys. **94**, 328 (2005).

[30] S. Zhao, G. Li, A. Ding, T. Wang, and Q. Yin, J. Phys. D. Appl. Phys. **39**, 2277 (2006).

[31] S. Saïd and J. P. Mercurio, J. Eur. Ceram. Soc. **21**, 1333 (2001).

[32] Y.S. Sung, J.M. Kim, J.H. Cho, T.K. Song, M.H. Kim, H.H. Chong, T.G. Park, D. Do, and S.S. Kim, Appl. Phys. Lett. **96**, 22901 (2010).

[33] Y.S. Sung, J.M. Kim, J.H. Cho, T.K. Song, M.H. Kim, and T.G. Park, Appl. Phys. Lett. **98**, 12902 (2011).

[34] P.V.B. Rao and T.B. Sankaram, Integr. Ferroelectr. **120**, 64 (2010).